

Effects of a topically applied wound ointment on epidermal wound healing studied by *in vivo* fluorescence laser scanning microscopy analysis

Bernhard Lange-Asschenfeldt

Charité-Universitätsmedizin Berlin
University Medical School
Department of Dermatology, Venerology and Allergology
and
Skin Cancer Center
Berlin, 10117
Germany
E-mail: bernhard.lange-asschenfeldt@charite.de

Alena Alborova

Charité-Universitätsmedizin Berlin
University Medical School
Department of Dermatology, Venerology and Allergology
and
Center of Experimental and Applied Skin Physiology
Berlin, 10117
Germany

Daniela Krüger-Corcoran

Charité-Universitätsmedizin Berlin
University Medical School
Department of Dermatology, Venerology and Allergology
and
Skin Cancer Center
Berlin, 10117
Germany

Alexa Patzelt

Heike Richter

Charité-Universitätsmedizin Berlin
University Medical School
Department of Dermatology, Venerology and Allergology
and
Center of Experimental and Applied Skin Physiology
Berlin, 10117
Germany

Wolfram Sterry

Charité-Universitätsmedizin Berlin
University Medical School
Department of Dermatology, Venerology and Allergology
Berlin, 10117
Germany

Axel Kramer

Ernst Moritz Arndt University Greifswald
Institute of Hygiene and Environmental Medicine
Greifswald, 17489
Germany

Eggert Stockfleth

Charité-Universitätsmedizin Berlin
University Medical School
Department of Dermatology, Venerology and Allergology
and
Skin Cancer Center
Berlin, 10117
Germany

Jürgen Lademann

Charité-Universitätsmedizin Berlin
University Medical School
Department of Dermatology, Venerology and Allergology
and
Center of Experimental and Applied Skin Physiology
Berlin, 10117
Germany

Abstract. Epidermal wound healing is a complex and dynamic regenerative process necessary to reestablish skin integrity. Fluorescence confocal laser scanning microscopy (FLSM) is a noninvasive imaging technique that has previously been used for evaluation of inflammatory and neoplastic skin disorders *in vivo* and at high resolution. We employed FLSM to investigate the evolution of epidermal wound healing noninvasively over time and *in vivo*. Two suction blisters were induced on the volar forearms of the study participants, followed by removal of the epidermis. To study the impact of wound ointment on the process of reepithelization, test sites were divided into two groups, of which one test site was left untreated as a negative control. FLSM was used for serial/consecutive evaluations up to 8 days. FLSM was able to visualize the development of thin keratinocyte layers developing near the wound edge and around hair follicles until the entire epidermis has been reestablished. Wounds treated with the wound ointment were found to heal significantly faster than untreated wounds. This technique allows monitoring of the kinetics of wound healing noninvasively and over time, while offering new insights into the potential effects of topically applied drugs on the process of tissue repair. © 2009 Society of Photo-Optical Instrumentation Engineers. [DOI: 10.1117/1.3213603]

Keywords: medicine; wound healing; biomedical optics; laser scanning microscopy.

Paper 09083R received Mar. 12, 2009; revised manuscript received Jun. 19, 2009; accepted for publication Jul. 6, 2009; published online Sep. 8, 2009.

1 Introduction

Tissue repair is a well-orchestrated process involving a variety of steps and signals necessary to reestablish tissue integrity.¹ The process of wound healing consists of an in-

Address all correspondence to: Bernhard Lange-Asschenfeldt, Charité-Universitätsmedizin Berlin, University Medical School, Department of Dermatology, Venerology and Allergology and Skin Cancer Center, 10117 Berlin, Germany. Tel.: +49 30 450 518728; Fax: +49 30 450 518928; bernhard.lange-asschenfeldt@charite.de

flammatory phase with wound exudation, a phase of proliferation and migration of tissue cells into the wound bed, and ultimately a phase of restoration of the epidermis with potential scarring following deeper dermal defects.² The human epidermis consists of several specialized keratinocyte cell layers that need to be fully restored for completion of the wound healing process.

A variety of assays are used to study the process of epidermal wound healing and potential effects of topical applied drugs on tissue repair. An evaluation of the morphological changes in skin wounds may be obtained by excisional biopsies from the wound site followed by histopathological examination using light microscopy. This technique allows a detailed analysis at high resolution but involves surgery and further laborious steps such as tissue processing, sectioning, and staining to permit conclusive interpretation. Furthermore, the removal of the tissue sample does not permit repeated analyses of the same wound site, thereby limiting the capability for evaluation of dynamic processes over time.

Several techniques suitable for real-time, noninvasive observations have been explored to study cutaneous tissue repair. Optical coherence tomography (OCT), high-frequency ultrasound (HFUS), magnetic resonance imaging (MRI), multispectral fluorescence polarization imaging, terahertz imaging, near-infrared, and Raman spectroscopy have been proven to be useful tools for the noninvasive analysis of skin physiology and cutaneous diseases.³⁻⁵

Recently, *in vivo* confocal microscopic techniques have been described for noninvasive analysis of human tissue *in vivo*. Among them, fluorescence confocal laser scanning microscopy (FLSM) allows the visualization of subsurface details in living human skin by means of optical sectioning.⁶ The principle of FLSM is based on the excitation and detection of fluorophores by means of scanning a focal plane within the tissue using a laser light source.⁶ The technique enables preservation of the tissue's physical structure and physiologic state *in vivo*, thereby allowing a sequential observation of dynamic skin processes such as inflammation or hyperproliferation at high resolution and in real time. While the resolution of FLSM is comparable to routine histological analysis, the optical penetration of FLSM is limited to the epidermis and upper dermis based on the penetration depth of the laser used.⁶ Compared to conventional histology, the major differences are that FLSM images are oriented horizontally to the skin surface (*en face*) and that they are analyzed in gray scale. Contrast and image interpretation is based on the presence of endogenous (autofluorescence) or exogenous fluorophores (fluorescent contrast agents). With respect to the system used in this investigation and for the purpose of this study, the use of exogenous fluorescent contrast agents was required to provide sufficient contrast within the tissue.⁷

The goal of this study was to evaluate the applicability of FLSM for the investigation of epidermal wound healing and the effects of topically applied wound ointment on epidermal tissue repair over a time course of 8 days.

2 Materials and Methods

2.1 Study Participants and Study Protocol

Six ($n=6$) individuals aged between 22 and 42 years with no history of skin diseases participated in the study after their

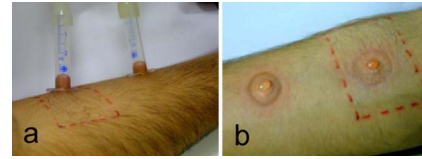


Fig. 1 Induction of suction blisters for the study of epidermal wounds. (a) Tubes of syringes pressed upside-down onto the skin. Next, the needle was connected to a vacuum pump applying a negative pressure at 0.3 bar for 60 min. (b). After the generation of the suction blisters, the vacuum pump was disconnected, and the roof of the blister representing the epidermis was removed.

written consent was obtained. All participants were recruited from the Department of Dermatology, Charité University Medicine, Berlin. All research was conducted according to the Declaration of Helsinki principle.

2.2 Methods of Epidermal Wounding

At day 0, two suction blisters were induced on the untreated volar forearms of the study participants. The blisters were established using the tubes of syringes pressed upside down onto the skin. Next, the needles were connected to a vacuum pump applying a negative pressure at 0.3 bar for 60 min (Fig. 1). Following the generation of the suction blisters, the vacuum pump was disconnected and the roof of the blister, corresponding to the full epidermal thickness was removed.

2.3 Treatment of Epidermal Wounds

After the removal of the epidermis, one of the two established wound sites on the forearm of the participants was treated twice a day with the wound ointment over a time period of 8 days. The remaining wound site remained untreated, subsequently serving as control site. During the entire duration of the study, all wound sites were covered with a self-adhesive wound dressing made of a soft nonwoven fabric as support material, with an absorbent wound dressing pad made of 100% absorbent cotton wool, covered with a nonadherent microgrid wound-contact layer. The wound dressing was changed twice a day after the investigation of the wound site. The ointment used for the studies consisted of dexpanthenol 5%, cera alba, paraffinum liquidum, aqua, cetyl alcohol, stearyl alcohol, almond oil, lanolin alcohol, petrolatum, glyceryl oleate, and ozokerite.

2.4 Evaluation of Epidermal Wound Healing

The time course of tissue repair was documented on days 1, 3, 5, 7, and 8 by FLSM followed by descriptive image analysis, combined with a photographic documentation of the clinical presentation over a time period of 8 consecutive days.

In order to analyze the progression of tissue repair, the process of wound healing was divided into three phases. Phase 1 was defined as the time point after the removal of the epidermal blister roof characterized by inflammation and wound exudation. In phase 2, the formation of the first layer of corneocytes was observed. Phase 3 describes the end of tissue repair with all reemerged layers of corneocytes and a reestablished skin barrier. The classification of the healing wounds into these three phases allowed the documentation of

differences in the advancement of tissue repair between the study groups—i.e., those treated with topical ointment versus the group of untreated wounds.

We determined the specific phase of wound healing for all six study participants on days 1, 3, 5, 7, and 8, and the means of the wound healing phase were calculated for each group for all investigated time points. To compare means of untreated and treated wounds, Student *t*-tests for paired data were performed.

2.5 Fluorescence Laser Scanning Microscopy (FLSM)

A commercially available fluorescence laser scanning microscope (Stratum, OptiScan Ltd., Melbourne, Australia) was used in this study. The technical details of this technique have been summarized in former publications.⁸

Coherent laser light from a 50-mW, air-cooled, 488-nm, single-line argon ion laser is focused onto the proximal end of a single-mode optical fiber. By focusing the laser light onto the fiber tip, the laser light will be coupled into, and propagated along, the optical fiber. The laser light emerges from the distal end of the optical fiber and is focused by the objective lens onto the tissue. Light emanating from the same focal point within the specimen and collected by the objective lens will be focused back onto the distal end of the optical fiber, and propagated back toward the laser light source. Once the returning light emerges from the proximal end of the optical fiber, it is separated from the illumination path using a beam-splitter (or dichroic mirror), and focused onto a photomultiplier tube for detection. Light that emanates from a point in the specimen that is outside the focal point of the objective lens will not be focused onto the distal tip of the optical fiber, and therefore will not be propagated to the detector, thus optically isolating the focal plane from the surrounding structures.

Fluorescent molecules within the specimen are excited to an electronic singlet state by absorption of the energy from the illuminating photons. When the excited fluorophore returns to its ground state, energy is released in the form of a photon. The emitted photon is of lower energy than the photons used to excite the fluorophore molecule (therefore at a longer wavelength). Thus, the light collected from the focal point in the specimen by the objective lens comprises both laser light backscattered from tissue structures (same wavelength as illumination source) and the longer wavelength emitted from the excited fluorophore molecules. As the returning fluorescence is a different wavelength (color) than the illumination source, a dichroic mirror is used to separate the light returning from the sample path from the illumination path. A fluorescence barrier filter is also placed in the light path between the dichroic mirror and the photodetector to block any reflected laser light, thus permitting only the longer wavelength fluorescent signal to pass through to the detector for measurement.

To facilitate further miniaturization and simplification of the optical light path, the Stratum employs a fused, biconical tapered fiber-optic coupler in place of the dichroic mirror and single optical fiber. A fiber-optic coupler is made from two lengths of optical fiber that are twisted together in the middle and heated so that they fuse together, resulting in four “arms.” When light travels down one arm toward the waist of the

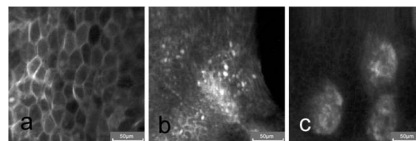


Fig. 2 FLSM findings of normal skin. (a) FLSM morphology of the upper skin keratinocyte layer, the *stratum corneum*. Corneocytes appear as polygonal cells. Due to the anucleated nature of corneocytes, fluorescein uptake is visible only in the surrounding intercellular spaces. (b) Representative image of the next deeper layer, *stratum spinosum*, 25 to 50 μm below the *stratum corneum*. Spinous keratinocytes appear as dark oval-shaped cells, while the intercellular spaces appear bright. (c) Basal keratinocytes are surrounding each papillary structure and appear darker than surrounding keratinocytes. The center of each papilla appears bright due to the abundance of collagen. Scale bars: 50 μm .

coupler, a proportion of the light can cross over into the other fiber at the coupler in a wavelength-dependent manner. Light will then emerge out of both exit arms of the coupler. The percentage of light emerging from each exit arm depends on the wavelength. This property is exploited to enable the signal returning from the specimen to be separated from the illumination path, thus eliminating the need for a dichroic beam-splitter, and reducing the total number of optical elements in the optical path of the instrument.

By scanning the focused point in a raster pattern over the specimen (point scanning), an array of point intensity measurements is collected from the area under investigation, and thus an image can be generated. In the Stratum, the focal point is moved over the field of view by physically moving the tip of the optical fiber within the scanner using *x* and *y* electromagnetic actuators. The imaging depth (*z* axis) in the sample is controlled by mechanically moving lens elements within the scanner to change the focal depth.

The maximum imaging depth in living tissue is up to approximately 300 μm and thereby restricted to the epidermis and superficial papillary dermis.

Fluorescence confocal microscopy relies on the differential distribution of endogenous (autofluorescence) or exogenous fluorescent molecules (fluorophores) within a tissue to produce contrast. Fluorescein sodium is a low molecular weight, water-soluble fluorescent contrast agent. Fluorescein has the advantages of high absorptivity, high quantum yield, and a peak maximum absorption, which closely matches the 488 nm spectral line of an argon ion laser. Topical and intradermal administration of fluorescein sodium (0.1% w/v solution) to the skin allows imaging of the superficial layers of the epidermis.

3 Results

3.1 Fluorescence Laser Scanning Microscopy Evaluation of Normal Skin

Overall, our findings are in agreement with former descriptions of normal healthy skin.⁶ While starting the imaging process from the skin surface and gradually progressing deeper along the *z* axis, the first images are obtained from the *stratum corneum* [Fig. 2(a)]. The anucleated cells are of polygonal shape and approximately 25 to 40 μm in size. The subjacent layer corresponds to the *stratum granulosum* and consists of

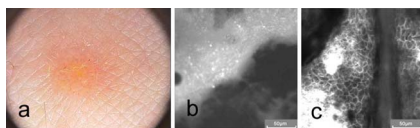


Fig. 3 Phase 1 of epidermal wound healing. (a) Close-up digital photograph of the epidermal wound immediately after the removal of the epidermis. Wound exudate dominates the appearance of the wound bed. (b) FLSM image focused on the wound edge. Wound exudation appears as a bright homogenous acellular area due to accumulating fluorescein (left upper border). (c) When focusing on the wound bed, the keratinocyte layer of the *stratum basale* and papillary structures are observed. The keratinocytes show an irregular shape after the mechanical removal of the upper epidermis. Scale bars: 50 μm .

two to four cell layers. Each cell is about 20 to 25 μm in size and presents with a central round to oval nucleus that appears as a well-demarcated structure of bright appearance within the cells. The cells of the *stratum spinosum* appear in a tight honeycombed pattern, with each cell measuring 15 to 20 μm in size separated from each other by distinct cell borders; nuclei appear as well-demarcated structures of bright appearance within the cells [Fig. 2(b)]. At the level of the basal and suprabasal layers, cells are seen as dark clusters, each measuring around 10 to 12 μm in size [Fig. 2(c)]. The dermoepidermal junction appears as round to oval rings of dark basal cells surrounding dermal papillae, which appear bright due to the homogenous distribution of the contrast agent in this layer [Fig. 2(c)].

3.2 Fluorescence Laser Scanning Microscopy Evaluation of Epidermal Wounds

Figure 3(a) shows a representative clinical photograph of an epidermal wound in phase 1. The exudate is visible as slightly yellowish superficial deposit. This encrusted exudate can be visualized by FLSM [Fig. 3(b)] on the surface of the skin and the wound edge. By focusing the evaluation on the central wound bed, the basal layer may be observed, since the epidermis has been mechanically removed. Figure 3(c) shows a typical image of the suprapapillary epidermal plate. The dermoepidermal junction appears as round to oval rings of dark cells measuring about 10 to 12 μm surrounding the bright dermal capillary loops.

In phase 2 of the wound healing process, clinical evaluation reveals that the wound bed is already covered by a thin layer of keratinocytes [Fig. 4(a)]. Corresponding FLSM evaluation demonstrates the presence of sparse clusters of corneocytes developing near the wound edge [Fig. 4(b)] and

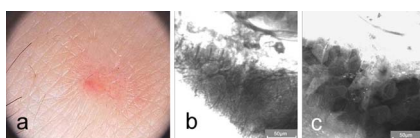


Fig. 4 Phase 2 of epidermal wound healing. (a) The wound bed is covered with the first layer of keratinocytes. (b) The first corneocytes are found at the wound edge growing into the epithelial defect. (c) Keratinocytes around hair follicles (dark gray, black) start to grow into the wound bed. Scale bars: 50 μm .

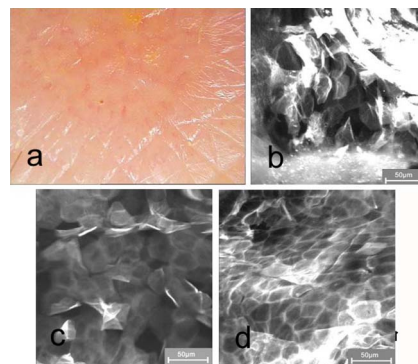


Fig. 5 Phase 3 of epidermal wound healing. (a) Close-up digital photography shows a completed tissue repair except the missing furrows of the epidermal skin. The wound is still partly covered with a small amount of encrusted exudate. (b) Several layers of polygonal corneocytes can be found at the entire wound site still showing an irregular shape. (c) At the level of the *stratum corneum*, bizarre-shaped, detached corneocytes resembling the aspect of keratinocytes are found in dry skin. (d) At the level of the *stratum granulosum*, a complete restoration of the typical honeycombed pattern can be observed. The complete restoration of the epidermis can also be validated by *in vivo* FLSM thickness measurements showing a thickness of $\sim 20 \mu\text{m}$ from the *stratum corneum* to the bordering *stratum granulosum*, corresponding to values of normal skin. Scale bars: 50 μm .

around hair follicles [Fig. 4(c)]. Phase 2 is completed after the formation of the first layer of corneocytes on the surface of the wound.

The clinical photograph of a representative wound in early phase 3 shows an almost reestablished skin surface aside from the ridges that are still missing [Fig. 5(a)]. Corresponding FLSM images reveal that the corneocytes in early phase 3 [Figs. 5(b) and 5(c)] do not appear as organized as seen in healthy skin [Fig. 2(a)], where corneocytes form a tight and uniform honeycomb pattern. Following FLSM evaluation in late phase 3, most corneocytes start to resume their uniform polygonal shape but still show uneven, bizarre-shaped corneocytes usually found in dry, chapped skin [Figs. 5(b) and 5(c)]. Figure 5(d) reveals an evenly distributed honeycombed pattern of uniform, polygonal-shaped corneocytes at the level of the *stratum granulosum*. Measurement of the entire epidermis at this time point using FLSM reveals the thickness of the normal epidermis adjacent to the former wound site, marking the completion of phase 3.

3.3 Effects of Topically Applied Wound Ointment on Epidermal Tissue Repair

Figure 6 depicts the average wound healing phase of topically treated and untreated wounds for all six study participants over a time course of 8 days. Interestingly, after the removal of the epidermal roof of the suction blister (phase 1), the formation of the first corneocyte layer (phase 2) occurs already around day 5 in the wound ointment-treated wound sites when compared to the untreated wound sites, where the corneocyte layer is not found before day 7. At the end of the experiment at day 8, all wounds treated with the ointment have reached phase 3, corresponding to a completely reestablished epidermis with all cell layers and a thickness comparable to the normal skin adjacent to the site of wounding. The

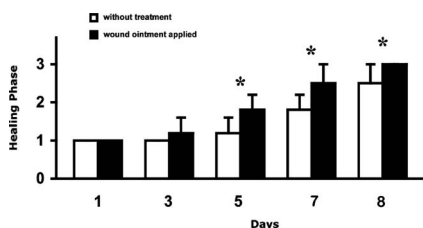


Fig. 6 Comparison of wound healing kinetics between treated and untreated wounds. Wounds were classified into three phases according to FLSM findings, as outlined in the Sec. 2. The specific phase of wound healing was determined for all six study participants, on days 1, 3, 5, 7, and 8, and the means of the wound healing phase were calculated for each group for all investigated time points. To compare the means of untreated and treated wounds, two-tailed Student *t*-tests for paired data were performed (significance level $*p < 0.05$). *x* axis corresponds to wound healing phase (1 to 3); *y* axis corresponds to days (investigated time points).

reestablishment of all epidermal cell layers was documented by FLSM imaging of each layer from the skin surface down to the basal cell layer and by obtaining thickness measurements of the epidermis using FLSM in comparison to normal skin.

4 Discussion

The final stage of wound healing following the event of a circumscribed epidermal defect is known as *restitutio ad integrum* of the injured tissue. This complex process of wound repair involves the organization of a multiplicity of cells localized at or recruited to the site of injury, including keratinocytes and various inflammatory cells. Their function is directed by an abundance of growth factors responsible for starting and directing the growth and organization of the migrating cells, while also providing stop signals for the newly developing tissue to prevent tissue hyperproliferation. At the same time, blood vessels play an inextricable role in controlling wound exudation and leukocyte recruitment before undergoing angiogenesis in order to meet the increased metabolic demand at the wound site.

The aim of investigating the process of tissue repair is to better understand this complex network of cell functions and to study the potential impact of exogenous or endogenous factors on cutaneous wound healing. Therefore, functional assays as well as morphometric methods are indispensable to evaluate these dynamic processes in a sequential manner. To date, a number of techniques have been used to study wound healing, the measurement of transepidermal water loss (TEWL) among the most established. The concept is based on the proposition that epidermal wounding corresponds to a compromised skin barrier, leading to an increased TEWL.^{9,10} Over time, TEWL values (expressed in $\text{g}/\text{m}^2/\text{h}$, see Ref. 9) of epidermal wounds are expected to decrease, since the development of an intact epidermis leads to a reconstitution of the epidermal barrier. However, the TEWL measurements can be easily influenced by wound exudation and scab formation, by perspiration of the study objects, and by any topically applied drugs or cosmetic products during investigation.

FLSM allows the visualization of the entire epidermis at cellular resolution, thereby distinguishing itself from other

noninvasive observational tools with low depth resolution such as optical coherent tomography.¹¹ Moreover, FLSM allows the repetitive investigation of the same wound site, contrasting with excisional skin biopsies evaluated by conventional histology.

Our FLSM findings concerning the imaging of normal skin are in agreement with previous reports.⁶ The observation of epidermal wound healing using FLSM underlined the significance and contribution of growing and migrating keratinocytes originating from the hair follicles remaining in the wound bed after an epidermal damage, since migrating keratinocytes were found within the first days surrounding almost all hair follicles. These findings are not surprising, since mesenchymal stem cells surround the hair follicle and are known to differentiate into a variety of epidermal cells such as keratinocytes.

However, newly formed epithelial cells can be difficult to identify, as they are partly translucent and may be hidden by slough, fibrous tissue, or exudate. FLSM seems to be a valuable tool in the observation of these freshly developed and thin layers of keratinocytes. The horizontal imaging technique of FSLM allows us to depict the very early clusters of keratinocytes organized as sheets of single-cell layers around hair follicles and at the wound edges. This advantage of FSLM over routine histology allows us to define this early state of wound healing as phase 2 and thereby enables the investigators to discriminate even subtle differences in the kinetics of wound healing between treated and untreated wound sites.

In our study, topical treatment of the wounds with a wound ointment leads to an accelerated wound healing compared to untreated controls as assessed by these early detectable phases of wound healing. Treated wounds entered the second and third healing phases days earlier than untreated wounds, showing a potential benefit of moist wound care.

Experimental evidence indicating that keeping wounds moist accelerates reepithelization is one of the major breakthroughs of the last 50 years^{12,13} and led to the development of a vast array of moisture-retentive dressings that promote moist wound healing.¹⁴

It is not clear whether moisture-retentive dressings work mainly by keeping the wound fluid in contact with the wound. For example, fluid collected from acute wounds stimulates the *in vitro* proliferation of fibroblasts, keratinocytes, and endothelial cells.^{15,16} However, corneocytes on the wound surface in our study showed the same appearance as corneocytes of dry skin, where the beneficial affects of wound ointment application is well investigated.

Wound ointment as used in our experiments consists of several ingredients, such as *cera alba*, *paraffinum liquidum*, almond oil, lanolin alcohol, and *petrolatum*, known to bind the moisture in dry skin as well as containing the wound exudate. Thus, the ointment forms a moist environment comparable to the moisture-retentive dressings that represent one of the most important components of modern wound management. For this reason, the application of wound ointments as used in our experiments could be a benefit for acute epidermal wounds with a moderate exudation level.

In summary, FLSM is a suitable technique for the noninvasive investigation of epidermal wound healing and potential effects of topically applied drugs or moisturizing aids. The definition of wound healing phases by morphological criteria

of the wound bed detectable by FLSM allows us to document potential differences in the kinetics of tissue repair.

Acknowledgments

We would like to thank the Skin Physiology Foundation of the Donor Association for German Science and Humanities for their financial support.

References

1. R. A. F. Clark, "Basics of cutaneous wound repair," *J. Dermatol. Surg. Oncol.* **19**, 693–706 (1993).
2. D. T. Rovee, *The Epidermis in Wound Healing*, Informa Health Care, London, (2004).
3. M. Vogt, A. Knüttel, K. Hoffmann, P. Altmeyer, and H. Ermert, "Comparison of high frequency ultrasound and optical coherence tomography as modalities for high resolution and noninvasive skin imaging," *Biomed. Tech.* **48**(5), 116–121 (2003).
4. F. Mirrashed and J. C. Sharp, "In vivo morphological characterization of skin by MRI micro-imaging methods," *Skin Res. Technol.* **10**(3), 149–160 (2004).
5. P. J. Caspers, G. W. Lucassen, E. A. Carter, H. A. Bruining, and G. J. Puppels, "In vivo confocal Raman microspectroscopy of the skin: noninvasive determination of molecular concentration profiles," *J. Invest. Dermatol.* **116**(3), 434–442 (2001).
6. L. D. Swindle, S. G. Thomas, M. Freeman, and P. M. Delaney, "View of normal human skin *in vivo* as observed using fluorescent fiber-optic confocal microscopic imaging," *J. Invest. Dermatol.* **121**(4), 706–712 (2003).
7. K. König, P. T. So, W. W. Mantulin, B. J. Tromberg, and E. Gratton, "Two-photon excited lifetime imaging of autofluorescence in cells during UVA and NIR photostress," *J. Microsc.* **183**(Pt 3), 197–204 (1996).
8. S. Astner, S. Gonzalez, and E. Gonzalez, "Noninvasive evaluation of allergic and irritant contact dermatitis by *in vivo* reflectance confocal microscopy," *Contact Dermatitis* **17**(4), 182–191 (2006).
9. J. J. Levy, J. von Rosen, J. Gassmuller, R. Kleine Kuhlmann, and L. Lange, "Validation of an *in vivo* wound healing model for the quantification of pharmacological effects on epidermal regeneration," *Dermatology (Basel, Switz.)* **190**(2), 136–141 (1995).
10. H. J. Weigmann, J. Ulrich, S. Schanzer, U. Jacobi, H. Schaefer, W. Sterry, and J. Lademann, "Comparison of transepidermal water loss and spectroscopic absorbance to quantify changes of the *stratum corneum* after tape stripping," *Skin Pharmacol. Appl. Skin Physiol.* **18**(4), 180–185 (2005).
11. J. Lademann, N. Otberg, H. Richter, L. Meyer, H. Audring, A. Teichmann, S. Thomas, A. Knüttel, and W. Sterry, "Application of optical noninvasive methods in skin physiology: a comparison of laser scanning microscopy and optical coherent tomography with histological analysis," *Skin Res. Technol.* **13**(2), 119–132 (2007).
12. G. D. Winter, "Formation of the scab and the rate of epithelization of superficial wounds in the skin of the young domestic pig," *Nature (London)* **193**, 293–294 (1962).
13. C. D. Hinman and H. Maibach, "Effect of air exposure and occlusion on experimental human skin wounds," *Nature (London)* **200**, 377–378 (1963).
14. L. G. Ovington, "Wound care products: how to choose," *Adv. Skin Wound Care* **14**(5), 259–266 (2001).
15. M. H. Katz, A. F. Alvarez, R. S. Kirsner, W. H. Eaglstein, and V. Falanga, "Human wound fluid from acute wounds stimulates fibroblast and endothelial cell growth," *Adv. Chem. Ser.* **25**(6 Pt 1), 1054–1058 (1991).
16. M. R. Schaffer, U. Tantry, G. M. Ahrendt, H. L. Wasserkrug, and A. Barbul, "Stimulation of fibroblast proliferation and matrix contraction by wound fluid," *Int. J. Biochem. Cell Biol.* **29**(1), 231–239 (1997).